

Large anisotropy in the paramagnetic susceptibility of SrRuO₃ films

Yevgeny Kats,* Isaschar Genish, and Lior Klein

Department of Physics, Bar-Ilan University, Ramat-Gan 52900, Israel

James W. Reiner[†] and M. R. Beasley

T. H. Geballe Laboratory for Advanced Materials, Stanford University, Stanford, California 94305, USA

(Received 13 October 2004; published 10 March 2005)

By using the extraordinary Hall effect in SrRuO₃ films we performed measurements of the paramagnetic susceptibility in this itinerant ferromagnet, from T_c (~ 150 K) to 300 K. These measurements, combined with measurements of magnetoresistance, reveal that the susceptibility, which is almost isotropic at 300 K, becomes highly anisotropic as the temperature is lowered, diverging along a single crystallographic direction in the vicinity of T_c . The results provide a manifestation of the effect of large magnetocrystalline anisotropy in the paramagnetic state of a $4d$ itinerant ferromagnet.

DOI: 10.1103/PhysRevB.71.100403

PACS number(s): 75.30.Gw, 72.25.Ba, 75.40.Cx, 75.50.Cc

The coupling of spin to electronic orbitals yields the ubiquitous phenomenon of magnetocrystalline anisotropy (MCA) in ferromagnets.¹ While the manifestation of MCA below T_c in the form of hard and easy axes of magnetization is well studied, the fact that the strength of the MCA decreases with temperature as a high power of the spontaneous magnetization² could give the impression that MCA effects above T_c are at most a weak perturbation. Here we show that the MCA has a significant effect in the paramagnetic state of the $4d$ itinerant ferromagnet SrRuO₃ over a wide range of temperatures—not only is the susceptibility diverging along a single axis at T_c , but the difference between the susceptibilities along the different crystallographic axes is noticeable ($>30\%$) already at $t \equiv (T - T_c)/T_c = 0.5$.

A paramagnetic susceptibility diverging along only one crystallographic direction has been reported previously for bulk specimens of Cu(NH₄)Br₄·2H₂O,³ but the anisotropy there was found to be only 2% of the exchange integral J (compared to $\sim 30\%$ which we find in SrRuO₃). Another report refers to two-dimensional cobalt films, where an anisotropy of 5% was measured.⁴ In both cases, the temperature range for which the susceptibility was measured is by an order of magnitude smaller (in units of T_c) than in our measurements of the three-dimensional SrRuO₃ films.

Measuring the paramagnetic susceptibility in films poses a considerable technical challenge due to the combination of small magnetic moment of the film with large background signal from the substrate. We avoided these difficulties by using the extraordinary Hall effect (EHE) whose signal depends on the film internal magnetization and not on the total magnetic moment of the sample. Therefore, the signal does not diminish with decreasing thickness, neither is it affected by the substrate magnetization.

We study epitaxial films of the itinerant ferromagnet SrRuO₃ grown by reactive electron-beam coevaporation⁵ on miscut ($\sim 2^\circ$) SrTiO₃ substrates. The orthorhombic unit cell ($a = 5.53$ Å, $b = 5.57$ Å, $c = 7.85$ Å) is slightly strained by the substrate,⁶ which seems to be the reason for the reduced T_c of the films ($T_c \sim 150$ K) relative to that of bulk single crystals ($T_c \sim 165$ K). In the ferromagnetic state, there is a

single easy axis of magnetization, roughly in the b direction.^{7,8} The films are single phase, with the $[110]$ direction perpendicular to the surface (as was shown by transmission electron microscopy study of films grown in the same apparatus⁷), so that the b direction is at 45° out of the plane of the film. For measurements of Hall effect, the films were patterned by photolithography, and we have subtracted data obtained at reversed fields to eliminate the field-symmetric contribution arising from longitudinal offset of the Hall leads. We studied films with thicknesses from 6 to 150 nm, and obtained almost thickness-independent results. The Hall-effect data presented below are from a 30-nm film.

The transverse electric field \mathbf{E}_H in magnetic conductors originates from both the *ordinary* (or *regular*) Hall effect (OHE), which depends on the magnetic induction \mathbf{B} , and the *extraordinary* (or *anomalous*) Hall effect (EHE), which depends on the magnetization \mathbf{M} ,

$$\mathbf{E}_H = -R_0 \mathbf{J} \times \mathbf{B} - R_s \mathbf{J} \times \mu_0 \mathbf{M},$$

where \mathbf{J} is the current density, R_0 is the ordinary Hall coefficient related to the carrier density n , and R_s is the extraordinary Hall coefficient which has been explored in the ferromagnetic phase of SrRuO₃ by temperature-dependent⁹ and field-dependent¹⁰ measurements. (Possible contribution of the *planar* Hall effect¹¹ is not considered, since it is eliminated in our subtraction procedure that leaves only field-antisymmetric contributions.)

In measurements above T_c we found that a significant Hall effect develops even when the magnetic field \mathbf{H} is applied parallel to the current which flows along the $[1\bar{1}0]$ direction. The temperature dependence of this Hall effect resembles the expected behavior of the induced magnetization (see Fig. 1). These results indicate that the measured Hall effect is an EHE related to an out-of-plane component of \mathbf{M} generated by in-plane \mathbf{H} . The fact that \mathbf{M} is not parallel to \mathbf{H} suggests anisotropic paramagnetic susceptibility.

For quantitative characterization of the susceptibility anisotropy, we measured the Hall effect as a function of field direction at various temperatures. For each temperature

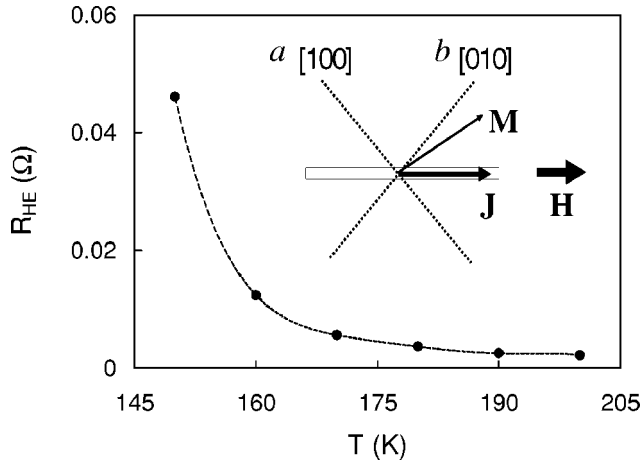


FIG. 1. Hall effect with $H=2500$ Oe applied parallel to the current (along the $[1\bar{1}0]$ direction) as a function of temperature above T_c (≈ 147 K). The dashed line is a guide to the eye.

above T_c , a small-field limit exists, where the magnetization depends linearly on the field and can be fully described in terms of constant susceptibilities χ_a , χ_b , and χ_c along the a , b , and c crystallographic directions, respectively ($\mu_0 M_a = \chi_a H_a$, etc). An example of measurements in this limit is shown in Fig. 2, where the EHE resistance ($R_{EHE} = \mu_0 R_s M_{\perp} / t$, where t is the thickness of the sample) is shown for two different fields at $T=153$ K as a function of the angle θ (see inset). The solid curve is a fit obtained by assuming certain values of χ_a and χ_b , based on the equation,

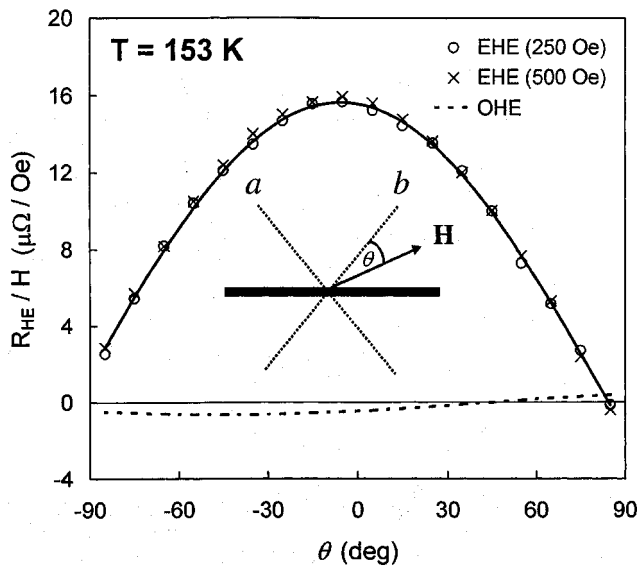


FIG. 2. EHE at $T=153$ K divided by the applied field H (circles: 250 Oe, crosses: 500 Oe) as a function of the angle θ between \mathbf{H} and the b direction (see illustration). The dashed curve is the OHE. The solid curve is a fit obtained by assuming certain constant values for the susceptibility along the a and b directions.

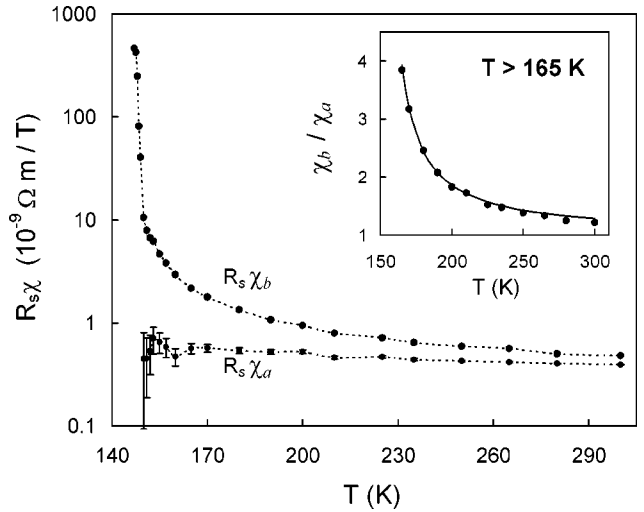


FIG. 3. Susceptibility along the crystallographic directions $[100]$ (χ_a) and $[010]$ (χ_b) as a function of temperature, on a semilog plot. The values are multiplied by R_s , whose temperature dependence is expected to be smooth. The error bars for $R_s \chi_a$ reflect an uncertainty of up to 2° in θ . The dashed lines are guides to the eye. The inset shows the ratio χ_b / χ_a for $165 \text{ K} < T < 300 \text{ K}$. The solid curve is a fit to $(T - T_{c,a}^{MF}) / (T - T_{c,b}^{MF})$ with $T_{c,a}^{MF} = 109 \text{ K}$, $T_{c,b}^{MF} = 150.5 \text{ K}$.

$$R_{EHE}(H, \theta) = \frac{R_s H}{\sqrt{2} t} (\chi_b \cos \theta - \chi_a \sin \theta).$$

Figure 2 also demonstrates the relatively small magnitude and different angular dependence of the OHE, which was subtracted from the measured signal.¹²

The main result of this paper is presented in Fig. 3, which shows the temperature dependence of the susceptibilities χ_a and χ_b (multiplied by R_s). We see that the susceptibility is very anisotropic throughout most of the investigated temperature range. Particularly, χ_b exhibits striking divergence at T_c , becoming several orders of magnitude larger than χ_a , while χ_a changes moderately. The actual divergence of χ_b is even stronger than shown in Fig. 3 since χ_b was not corrected for the demagnetizing field (because of uncertainty in the value of R_s); consequently, the apparent susceptibility in our measurement configuration is only $\chi_b / (1 + \chi_b / 2)$.

Since the c direction is in the plane of the film, the EHE measurement could not be used to determine χ_c (the insensitivity of EHE to a field component in the c direction was experimentally confirmed). Therefore, measurements of magnetoresistance (MR) $\Delta\rho \equiv \rho(H) - \rho(0)$ were employed.¹³ Based on previous¹⁴ and current results (see inset to Fig. 4), $\Delta\rho \propto -M^2$ (for a constant direction of magnetization). Thus we can infer the susceptibility behavior along a , b , and c directions by comparing the MR obtained with fields applied along these directions. The results, shown in Fig. 4, clearly indicate that the induced magnetization along the b direction grows as T_c is approached much more rapidly than along the a or c directions. The divergence here is less pronounced than in Fig. 3 since for fields applied here the magnetization along b is sublinear (but using lower fields would not allow us to obtain accurate MR data for the a and c directions). The

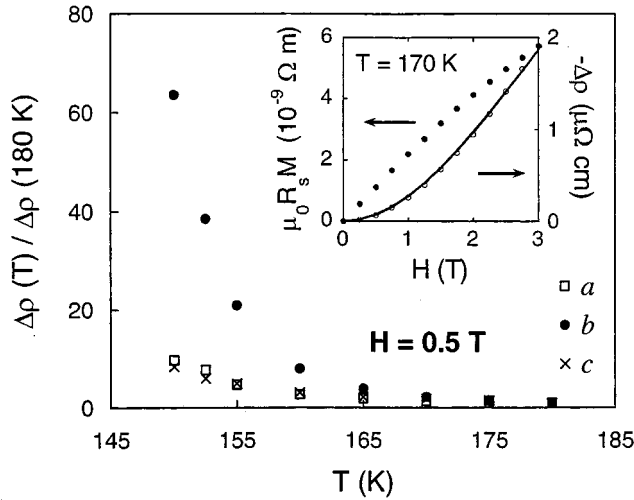


FIG. 4. Magnetoresistance as a function of temperature with a field of 0.5 T applied along the different crystallographic directions (the values are normalized to the values at 180 K). The inset shows the magnetization ($\mu_0 R_s M$) and magnetoresistance ($\Delta\rho$) as a function of a field (applied along the b direction, at $T=170$ K). The solid curve is a fit to $\Delta\rho \propto -M^2$.

temperature dependence of the MR with $\mathbf{H} \parallel c$ is very similar to the MR with $\mathbf{H} \parallel a$, suggesting that the behavior of χ_c is similar to the behavior of χ_a .

The data in Figs. 3 and 4 imply that only the susceptibility along the b direction (which is also the easy axis of the spontaneous magnetization^{7,8}) diverges at the phase transition; moreover, the large anisotropy of the susceptibility is noticeable ($>30\%$) already at $t \equiv (T - T_c)/T_c = 0.5$.

Anisotropy in the behavior of the susceptibility arising from MCA may be described microscopically by a Heisenberg model with *anisotropic exchange*,

$$\mathcal{H} = - \sum_{\langle ij \rangle, \alpha} J_{\alpha} S_{i\alpha} S_{j\alpha} \quad (1)$$

or with *single-site anisotropy*,

$$\mathcal{H} = -J \sum_{\langle ij \rangle} \mathbf{S}_i \cdot \mathbf{S}_j - \sum_{i, \alpha} D_{\alpha} S_{i\alpha}^2, \quad (2)$$

where $\alpha = a, b, c$ denotes spin components along the crystal-line directions, and i, j denote lattice sites. Band calculations¹⁵ and spin-polarization measurements¹⁶ show that SrRuO₃ is an itinerant ferromagnet. However, various theoretical models (e.g., the local-band theory¹⁷) indicate that magnetic moments in itinerant ferromagnets can behave as if localized even above T_c , thus vindicating the description of their magnetic interactions by the Heisenberg Hamiltonian. The experimental observation that the exchange splitting in SrRuO₃ does not change much as T_c is approached¹⁸ supports the relevance of such a treatment to SrRuO₃.

Since $T_c \propto J$, anisotropic exchange results in a different effective T_c for each spin component. Consequently, the susceptibility along the direction with the largest J diverges at the actual T_c , while no divergence occurs for the other spin components at any temperature.¹⁹ Single-site anisotropy

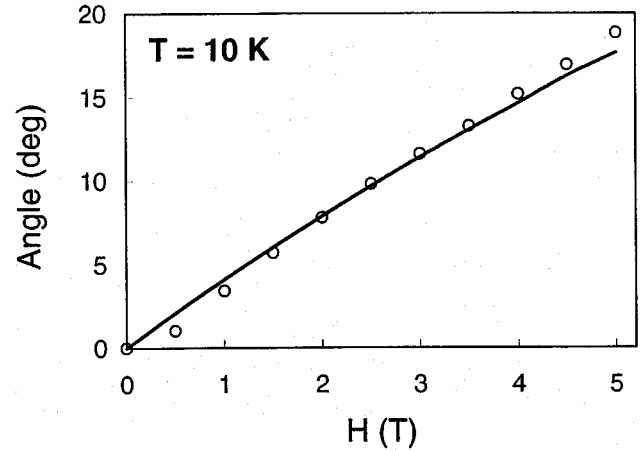


FIG. 5. Deviation of the magnetization from the easy axis as a function of the field which is applied at 60° relative to the easy axis. The solid curve presents the expected behavior with an anisotropy constant of 1.2×10^7 erg/cm³.

yields the same critical behavior,¹⁹ with an effective $\Delta J = \Delta D/z$, where z is the number of nearest neighbors.

The anisotropy ΔJ (or ΔD) can be estimated from the susceptibilities in the mean-field region, which are expected to follow the Curie-Weiss $1/(T - T_c^{MF})$ law (with a different mean-field transition temperature T_c^{MF} for each direction), if Pauli paramagnetism and diamagnetism can be neglected.²⁰ We cannot fit $R_s \chi_a$ or $R_s \chi_b$ as a function of temperature because the temperature dependence of R_s is unknown. However, the ratio χ_b/χ_a does not depend on R_s , and fitting the data to the expression $(T - T_{c,a}^{MF})/(T - T_{c,b}^{MF})$ converges to the values $T_{c,a}^{MF} = 109 \pm 2$ K, $T_{c,b}^{MF} = 150.5 \pm 0.5$ K for $165 \text{ K} < T < 300$ K (see inset in Fig. 3). From these values we find an anisotropy of $J_b - J_a \approx 0.3 J_{avg}$ or $D_b - D_a \approx 0.3 Jz$.

To examine whether the paramagnetic anisotropy is consistent with the ferromagnetic anisotropy we performed magnetization measurements below T_c . However, noting that the easy axis of the magnetization, which is along the b direction close to T_c , changes its orientation as the temperature is lowered (by a maximum of 15° at zero temperature)²² and considering that additional factors become significant when the magnetization is large, the most we can expect is an order-of-magnitude agreement between the paramagnetic and the ferromagnetic anisotropy.

Using a superconducting quantum interference device (SQUID) magnetometer which measures the whole magnetization vector, we estimated the ferromagnetic anisotropy by measuring the rotation of \mathbf{M} resulting from applying a magnetic field in the $[1\bar{1}0]$ direction. We find, between 10 and 90 K, a smooth rotation of \mathbf{M} in the (001) plane by up to $\sim 20^\circ$ at $H = 5$ T (see Fig. 5) almost without change of magnitude.²³ This behavior can be described by an anisotropy energy, $E_{anis} = K \sin^2 \theta$, with a weakly temperature-dependent anisotropy constant K whose low-temperature value is $(1.2 \pm 0.1) \times 10^7$ erg/cm³.

The large anisotropy constant [compared to 5×10^5 erg/cm³ in Fe, (Ref. 24), 8×10^5 erg/cm³ in Ni, (Ref. 25), and 4×10^6 erg/cm³ in hcp Co (Ref. 26)] is prob-

ably a result of the reduced symmetry²⁷ (orthorhombic) and the large spin-orbit coupling²⁸ through which the spin direction is affected by the crystal structure.

To relate the ferromagnetic anisotropy with Eqs. (1) and (2), we note that at low temperature the exchange aligns the spins along a single direction, thus the energy cost of magnetization rotation from the b direction toward the a direction by an angle θ in the case of anisotropic exchange is $\Delta E = zNS^2(J_b - J_a)\sin^2\theta$, where N is the number of spins per unit volume. A similar result is obtained in the case of single-site anisotropy. Considering that the zero-temperature magnetization is $1.4\mu_B$ per Ru ion, and calculating J according to the relation $J = 3k_B T_c^{MF} / 2zS(S+1)$, we obtain $J_b - J_a \approx 0.1J_{avg}$. This result is in reasonable agreement with $J_b - J_a \approx 0.3J_{avg}$ extracted from the anisotropic susceptibility.

Finally, we would like to note that while it is common to use the EHE as an indicator of magnetization, it is seldom used for a quantitative analysis of magnetic behavior. In this work we presented a striking example of the latter, by performing sensitive measurements of the zero-field-limit magnetic susceptibility in thin films of SrRuO₃, which allowed us to gain microscopic insight into the effect of MCA in the paramagnetic state of a $4d$ itinerant ferromagnet.

We would like to thank V. Kosoy for illuminating discussions, and A. Aharony, J. S. Dodge, and M. Gitterman for useful comments on the manuscript. We acknowledge support from the Israel Science Foundation funded by the Israel Academy of Sciences and Humanities.

*Present address: Department of Physics, Harvard University, Cambridge, MA 02138, USA.

†Present address: Department of Applied Physics, Yale University, New Haven, CT 06520-8284, USA.

¹C. Kittel, *Introduction to Solid State Physics* (Wiley, New York, 1986), p. 450.

²H. B. Callen and E. Callen, *J. Phys. Chem. Solids* **27**, 1271 (1966).

³H. Suzuki and T. Watanabe, *J. Phys. Soc. Jpn.* **30**, 367 (1971).

⁴P. J. Jensen, S. Knappmann, W. Wulfhekkel, and H. P. Oepen, *Phys. Rev. B* **67**, 184417 (2003).

⁵S. J. Benerofe *et al.*, *J. Vac. Sci. Technol. B* **12**, 1217 (1994).

⁶C. B. Eom, R. J. Cava, R. M. Fleming, J. M. Phillips, R. B. van Dover, J. H. Marshall, J. W. P. Hsu, J. J. Krajewski, and W. F. Peck, Jr., *Science* **258**, 1766 (1992).

⁷A. F. Marshall *et al.*, *J. Appl. Phys.* **85**, 4131 (1999).

⁸L. Klein *et al.*, *J. Phys.: Condens. Matter* **8**, 10111 (1996).

⁹M. Izumi, K. Nakazawa, Y. Bando, Y. Yoneda, and H. Terauchi, *J. Phys. Soc. Jpn.* **66**, 3893 (1997); L. Klein, J. W. Reiner, T. H. Geballe, M. R. Beasley, and A. Kapitulnik, *Phys. Rev. B* **61**, R7842 (2000).

¹⁰Y. Kats, I. Genish, L. Klein, J. W. Reiner, and M. R. Beasley, *Phys. Rev. B* **70**, 180407(R) (2004).

¹¹C. Goldberg and R. E. Davis, *Phys. Rev.* **94**, 1121 (1954); T. R. McGuire and R. I. Potter, *IEEE Trans. Magn.* **11**, 1018 (1975).

¹² R_0 was determined at $T \approx 130$ K by the method described in Ref. 10. While small changes in R_0 as a function of temperature cannot be excluded, our main results would be affected very little by such changes.

¹³The MR in SrRuO₃ is negative and related to suppression of spin-dependent scattering. Only at very low temperatures positive Lorentz magnetoresistance appears.

¹⁴Y. Kats, L. Klein, J. W. Reiner, T. H. Geballe, M. R. Beasley, and A. Kapitulnik, *Phys. Rev. B* **63**, 054435 (2001).

¹⁵G. Santi and T. Jarlborg, *J. Phys.: Condens. Matter* **9**, 9563 (1997).

¹⁶D. C. Worledge and T. H. Geballe, *Phys. Rev. Lett.* **85**, 5182 (2000); B. Nadgorny, M. S. Osofsky, D. J. Singh, G. T. Woods, R. J. Soulen, Jr., M. K. Lee, S. D. Bu, and C. B. Eom, *Appl.*

Phys. Lett. **82**, 427 (2003); P. Raychaudhuri, A. P. Mackenzie, J. W. Reiner, and M. R. Beasley, *Phys. Rev. B* **67**, 020411(R) (2003).

¹⁷V. Korenman, J. L. Murray, and R. E. Prange, *Phys. Rev. B* **16**, 4032 (1977).

¹⁸J. S. Dodge, E. Kulatov, L. Klein, C. H. Ahn, J. W. Reiner, L. Mieville, T. H. Geballe, M. R. Beasley, A. Kapitulnik, H. Ohta, Yu. Uspenskii, and S. Halilov, *Phys. Rev. B* **60**, R6987 (1999).

¹⁹P. Pfeuty and G. Toulouse, *Introduction to the Renormalization Group and to Critical Phenomena* (Wiley, New York, 1977), Chap. 8.

²⁰The Pauli paramagnetism and diamagnetism in SrRuO₃ are approximately 10% of the susceptibility at 300 K (Ref. 21). It is not clear whether their contribution to the EHE should go with the same R_s . If the same R_s is assumed, taking them into account does not have a significant effect on the result or the quality of the fit.

²¹G. Cao, S. McCall, M. Shepard, J. E. Crow, and R. P. Guertin, *Phys. Rev. B* **56**, 321 (1997).

²²This feature has been reported previously (Ref. 8) and it does not depend on film thickness. It is not due to the shape anisotropy, which is small ($M_s^2 \approx 5 \times 10^4$ erg/cm³ $\ll K$).

²³The contribution of the substrate was subtracted based on measurements of a bare substrate. Its signal is mainly diamagnetic, being for $H = 5$ T about 20% of the ferromagnetic signal of the 150-nm film which was measured.

²⁴C. D. Graham, Jr., *Phys. Rev.* **112**, 1117 (1958).

²⁵R. M. Bozorth, *Ferromagnetism* (Van Nostrand, New York, 1951), p. 569.

²⁶D. Weller, G. R. Harp, R. F. C. Farrow, A. Cebollada, and J. Sticht, *Phys. Rev. Lett.* **72**, 2097 (1994).

²⁷A remarkable example of the dependence of MCA on the crystal symmetry is the order-of-magnitude difference in the anisotropy constants between hcp and fcc Co (Ref. 26).

²⁸The SOC constant ζ in Ru ion (~ 900 cm⁻¹) is significantly larger than, for example, in Fe (~ 400 cm⁻¹), Ni (~ 600 cm⁻¹), and Co (~ 500 cm⁻¹). See: J. S. Griffith, *The Theory of Transition-Metal Ions* (Cambridge University Press, Cambridge, 1971), pp. 437–439.